



UNIVERSITY OF LEEDS

This is a repository copy of *Presence of ϵ and ϵ crystal structures in rapidly solidified intermetallic compound Ni₅Ge₃.*

White Rose Research Online URL for this paper:
<https://eprints.whiterose.ac.uk/178053/>

Version: Accepted Version

Article:

Haque, N, Jegede, OE and Mullis, AM orcid.org/0000-0002-5215-9959 (2021) Presence of ϵ and ϵ crystal structures in rapidly solidified intermetallic compound Ni₅Ge₃. Journal of Alloys and Compounds, 887. 161465. ISSN 0925-8388

<https://doi.org/10.1016/j.jallcom.2021.161465>

© 2021, Elsevier. This manuscript version is made available under the CC-BY-NC-ND 4.0 license <http://creativecommons.org/licenses/by-nc-nd/4.0/>.

Reuse

This article is distributed under the terms of the Creative Commons Attribution-NonCommercial-NoDerivs (CC BY-NC-ND) licence. This licence only allows you to download this work and share it with others as long as you credit the authors, but you can't change the article in any way or use it commercially. More information and the full terms of the licence here: <https://creativecommons.org/licenses/>

Takedown

If you consider content in White Rose Research Online to be in breach of UK law, please notify us by emailing eprints@whiterose.ac.uk including the URL of the record and the reason for the withdrawal request.



eprints@whiterose.ac.uk
<https://eprints.whiterose.ac.uk/>

Presence of ϵ and ε crystal structures in rapidly solidified intermetallic compound Ni_5Ge_3

Nafisul Haque^{1,2}, Oluwatoyin Enitan Jegede¹, Andrew M. Mullis¹

¹School of Chemical & Process Engineering, University of Leeds, Leeds LS2 9JT, UK

²Department of Metallurgical Engineering, NEDUET, University Road, Karachi - 75270

engrnafis@gmail.com, pmoej@leeds.ac.uk, A.M.Mullis@leeds.ac.uk

Abstract

The congruently melting, single phase intermetallic Ni_5Ge_3 has been subject to rapid solidification via drop-tube processing wherein powders, with diameters between > 850 to $150 \mu\text{m}$, are produced. At low cooling rates ($> 850 \mu\text{m}$ diameter particles, $< 700 \text{ K s}^{-1}$) the dominant solidification morphology, revealed after etching, is that of partial plate and lath microstructure in an otherwise featureless matrix. At slightly high cooling rates ($850 - 150 \mu\text{m}$ diameter particles, $700 - 7800 \text{ K s}^{-1}$) complete plate & lath microstructure observed, again imbedded within a featureless matrix. Selected area diffraction analysis in the TEM reveals that partial plate & lath are the disordered form of ϵ - Ni_5Ge_3 in a matrix of the ordered (double-superlattice) form. Partial plate & lath has a very different EBSD to the plate & lath structure. Histogram of the correlated grain orientation angle distribution across grain orientation in partial plate & lath microstructure sample from the $> 850 \mu\text{m}$ fraction showing random grain orientation. However, grain orientation in plate & lath structure from $300 - 212 \mu\text{m}$ fraction displaying the distribution predominance of low angle grain boundaries.

Keywords: rapid solidification; intermetallic compound; plate & lath microstructure.

1. Introduction:

There has been heightened interest in rapid solidification studies in recent times due to the fast progress made in additive manufacturing techniques in which precise control of solidification microstructures and defects is crucial for the performance and quality of the product [1]. Hence studies on rapid solidification and non-equilibrium processing are crucial in physical metallurgy and material science due to their potential to influence microstructural refinement, non-equilibrium phase formation and extend solid solubility,

enabling design of alloys with varied compositions and improved properties. Duwez [2] pioneered the rapid solidification of amorphous metals in the Au-Si system. Jones [3] and Boettinger [4] were also able to use the rapid solidification method to cause grain size [3] and micro segregation [4] refinement in various alloys. These refinements have also been said to improve physical properties of alloys: increases in yield and ultimate strength being reported by Jones [3], Taub and Jackson reported that rapid solidification could also lead to increased toughness [5], while Kang *et al.*, reported an increase in resistance to corrosion [6].

Knowledge of crystal structure is an essential pre-requisite for the understanding and alteration of structure-property relationship. The nature of bonding in intermetallic compound is a mixture of ionic, covalent and metallic bonding, with the atoms of the individual elements commence in a preferred position within the crystal lattice, which is referred to as ordering. The chemical ordering of intermetallic compounds is referred to as having the arrangement of same element in the lattice parameter, otherwise chemically disordered crystal structure will be formed. The Intermetallic compounds, Ni₃Al, Ni₃Si, Ni₃Fe and Ni₃Ge have an ordered L1₂ (cP4) crystal structure and have a space group 221. The intermetallic compound ε-Ni₅Ge₃ (high temperature) has the P6₃/mmc crystal structure (hexagonal, space group 194), while ε'-Ni₅Ge₃ (low temperature) has the C2 crystal structure (monoclinic, space group 5) [7]. The phase diagram of Ge – Ni system are shown in Figure 1 [8]. Where, the regions of ε-Ni₅Ge₃ and ε'-Ni₅Ge₃ are indicated with blue and green arrows respectively.

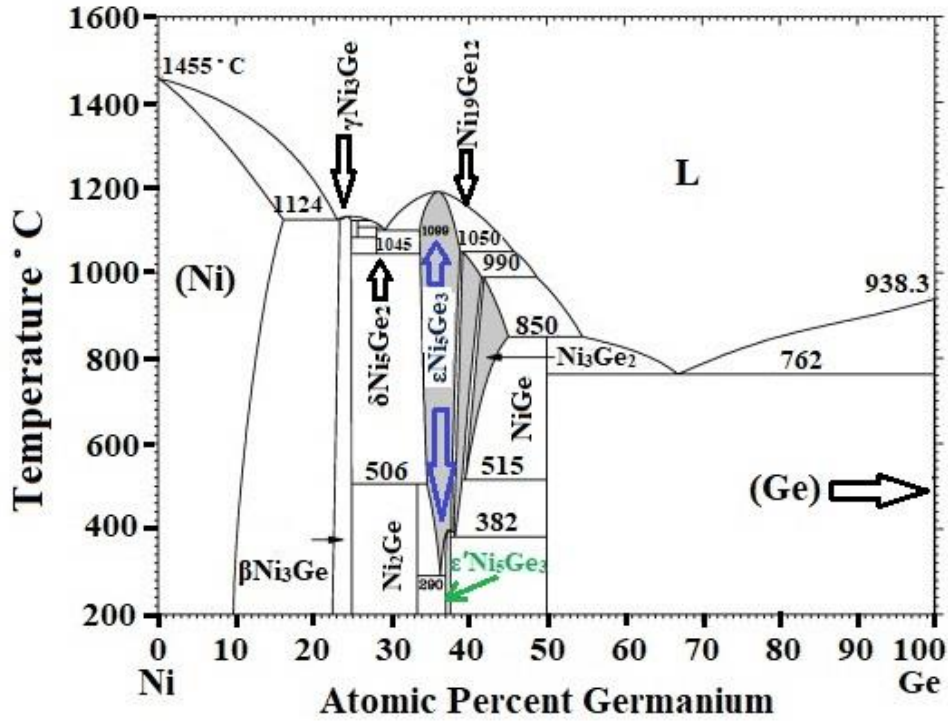


Figure 1: Ge - Ni phase diagram, after reproduced [8]

In intermetallic compounds [9-11], structures of a plate and lath generously are fairly common. Likewise, it is also common in some iron alloys [12]. A plate & lath structures was observed in γ -TiAl (Hyman *et al.*) [9]. It is stated that this resulted from α dendrites transforming into solid-state during cooling, which was done to a mixture of $\alpha_2 + \gamma$ laths that γ segregates enveloped. Plate and lath morphology were also observed in α_2 -Ti₃Al (McCullough *et al.*). As ϵ -Ni₅Ge₃, α_2 -Ti₃Al shares the P6₃/mmc space group [10].

In this article we present an analysis of rapidly solidified Ni-37.2 at%. Ge produced using the drop-tube technique. Rapid solidification was affected via drop-tube processing, wherein powders, with diameters between > 850 to 150 μ m, are produced.

Experimental Methods

The congruently melting ϵ -Ni₅Ge₃ compound occurs over the homogeneity range of 33.6 to 42.2 at. % Ge. ϵ -Ni₅Ge₃ and has the ordered hexagonal P6₃/mmc crystal structure [13]. ϵ -Ni₅Ge₃ was made via arc-melting elemental Nickel and Germanium together under a protective argon (Ar) atmosphere. XRD analysis using a PANalytical Xpert Pro X-Ray diffractometer was conducted to verify the phase composition of the subsequent ingot. The

drop tube apparatus worked under controlled heating and inert-gas vacuum system. It has the ability to produce a fine spray of droplets with undercooled metallic powder samples. In the drop tube apparatus, likely heterogeneous nucleation needs to be minimised by eliminating contaminants and impurities from the atmosphere in order to maximise undercooling. This is possible through a vacuum system made up of backfilled with nitrogen/helium, a sealed 6.5 m long chamber of drop tube, which has an integrated induction furnace, which has an induction coil connected to a RF generator at the top of the chamber. A pressurised gas system is also attached with the drop tube for the ejection of molten sample, which produces a final sample in the form of fine spray droplets powder. The sample was weighed following removal from the drop-tube and sieved into the size fractions; $> 850 \mu\text{m}$, to $150 \mu\text{m}$. For each size fraction the cooling rate, calculated using the methodology described in [14].

In this article we present our results for the $> 850 \mu\text{m} - 150 \mu\text{m}$ drop-tube samples. XRD analysis was performed on the drop-tube powders in order to check that the material remained single phase during subsequent processing. Following production the drop-tube the powders were mounted and polished to a $1 \mu\text{m}$ surface finish for microstructural analysis. A $0.1 \mu\text{m}$ colloidal silica suspension was used to obtain the high-quality surface finish required for EBSD analysis. A Carl Zeiss EVO MA15 scanning electron microscope (SEM) was used for metallographic analysis. A combination of equal parts HF, HCl and HNO_3 was used to perform the etching of samples. In order to confirm the chemical homogeneity of samples, an Oxford Instrument X-Max Energy-Dispersive X-Ray (EDX) detector was utilised. A FEI Quanta 650 FEGSEM with Oxford/HKL Nordlys EBSD system was used to perform Electron Back-Scatter Diffraction (EBSD) on unetched samples. An FEI Tecnai TF20 Transmission electron microscope (TEM) was also used to identify the internal structure (ordered or disordered) of partial plate & lath and complete lath & plate structure. Samples were prepared for TEM analysis by FEI Nova 200 nano-lab Focus ion beam (FIB).

2. Results and discussion

The arc-melted ingot of single phase Ni_5Ge_3 compound was rapidly solidified via drop-tube processing and powders obtained in the size range $> 850 \mu\text{m}$ to $150 \mu\text{m}$. Firstly, EDX

analysis was carried out on freshly polished samples to ensure the chemical composition of the all ranges of drop-tube samples. For this, EDX area scanning was randomly performed at least 10 particles of all ranges of drop-tube samples ($> 850 \mu\text{m}$ to $150 \mu\text{m}$) and measured chemical compositions were within the homogeneity range Ni – 37.2 at. % Ge [8]. Consequently, all ranges of drop-tube particles have the average chemical composition within the range of single phase, congruently melting compound, $\epsilon\text{-Ni}_5\text{Ge}_3$.

Samples from arc melted and all sieve fractions ($> 850 \mu\text{m}$ to $212 \mu\text{m}$) have also been subject to XRD analysis, with representative results being shown in **Figure 2**. By comparison with the ICDD reference patterns for $\epsilon\text{-Ni}_5\text{Ge}_3$ (04 – 004 – 7364) and $\epsilon'\text{-Ni}_5\text{Ge}_3$ (01-075-6729), confirms that the material remain fully single phase Ni_5Ge_3 , irrespective of the imposed cooling rate. In this way, the largest sieve fraction ($> 850 \mu\text{m}$) of this material was ϵ' , while those smaller than $850 \mu\text{m}$ ($850 \mu\text{m} - 150 \mu\text{m}$) were ϵ . Here, ϵ' is the equilibrium low temperature phase and ϵ a retained high temperature phase.

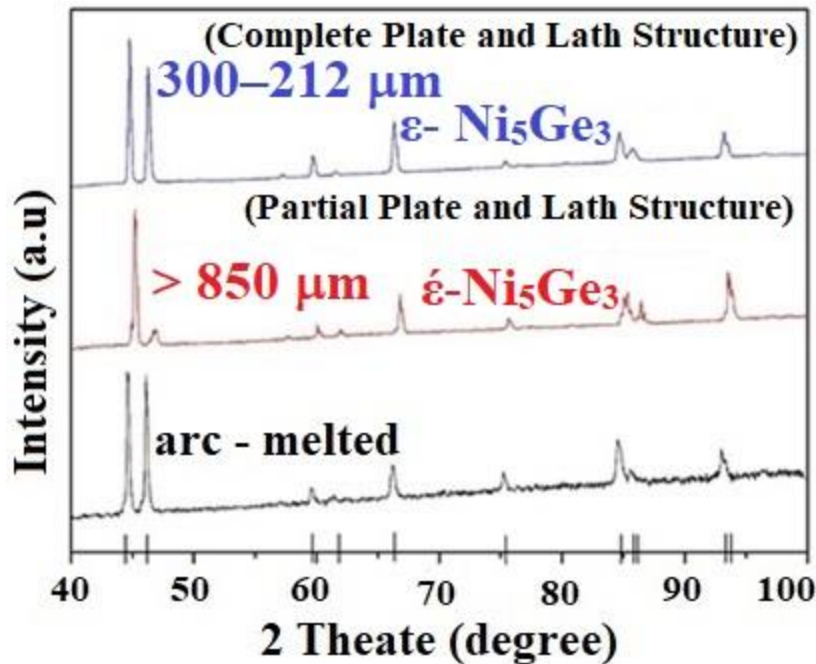
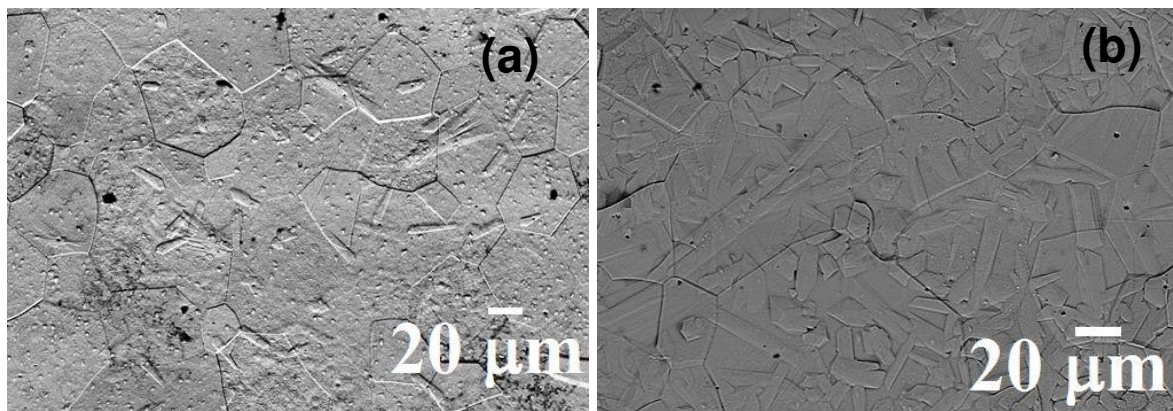


Figure 2: X – ray diffraction analysis of as cast (arc-melted) sample prior to drop-tube process (black), rapidly solidified sample (drop-tube processed) powder in the $>850 \mu\text{m}$ diameter particles (red) and $300 - 212 \mu\text{m}$ diameter particles (blue) respectively.

SEM was used for studying microstructures of the rapidly solidified Ni_5Ge_3 droplets, ranges from $> 850 \mu\text{m}$ to $150 \mu\text{m}$ sieve size fractions. Two different microstructures were observed. First, partial plate and lath type structures (**Figure 3a**) were observed at low cooling rates ($< 700 \text{ K s}^{-1}$, $> 850 \mu\text{m}$ diameter particles). Then, complete plate and lath type structure (**Figure 3b**) at high cooling rates ($700 - 7800 \text{ K s}^{-1}$, $850 - 150 \mu\text{m}$ diameter particles). Nevertheless, in other materials that display the plate and lath structure, such as Ti_3Al , it is apparent that this specific morphological composition is caused by the differences in phases that are contrasting.

The material being discussed here is single phase, so it is clearly a different case. In the case of a congruently melting compound the contrast would not be expected to arise from solid composition differences. The absence of solute partitioning is established in **Figure 3c**. This figure displays an EDX line scan that goes across a part of the isolated plate and lath morphology. From this we can deduce that, within the technique's experimental error, only small compositional variations exist between the surrounding matrix that is without features and the structures revealed by etching. Consequently, the contrast that is shown by the etching process does not appear to be related to differences in the phase composition of the samples. Nor does it appear to be related to the EDX chemical composition.



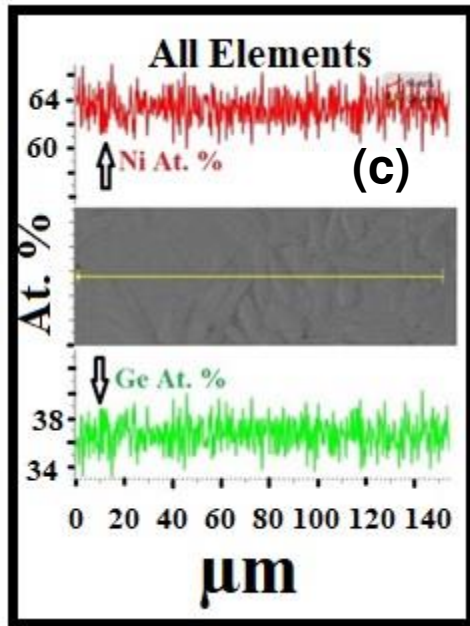


Figure 3: (a) SEM micrograph of HF etched Ni_5Ge_3 drop-tube particle from (a) the $> 850 \mu\text{m}$ size fraction showing numerous partial plate & lath structures (b) from the $300 - 212 \mu\text{m}$ size fraction showing complete plate & lath structures in a more-or-less featureless matrix and (c) EDX line scan across the diameter of droplet from the $300 - 212 \mu\text{m}$ size fraction, showing that the contrast revealed by etching is not the result of solute partitioning.

EBSD Euler map was used to study the grain structures of observed microstructure (partial plate and lath and complete plate and lath structure). For this, drop-tube sieve size fractions $> 850 \mu\text{m}$ to $150 \mu\text{m}$ ranges have been undertaken on freshly prepared samples, polished using $0.1 \mu\text{m}$ colloidal silica and without etching. The grain structure for the $> 850 \mu\text{m}$ to $150 \mu\text{m}$ sample are very clearly revealed in the EBSD Euler map, as an example of two selective size fractions $> 850 \mu\text{m}$ and $300 - 212 \mu\text{m}$ of partial plate & lath and complete plate and lath microstructure samples are shown in the **Figure 4a & 4c** respectively. The EBSD images show no evidence of either the partial plate & lath or complete plate & lath morphologies visible in the SEM images. Also, it suggests that the plate and laths have the same crystallographic orientation as the background. For the partial plate and lath microstructure sample size fractions $> 850 \mu\text{m}$, the orientation of each grain relative to its neighbours are largely random with some additional components of high angle as shown by the histogram of grain orientations in the **Figure 4b**. In contrast, for the complete

plate and lath microstructure sample size fractions 300 – 212, the orientation of grain relative to its neighbours are looks predominantly low angle grain boundaries (LAGB) as shown by the histogram of grain orientations in the **Figure 4d**.

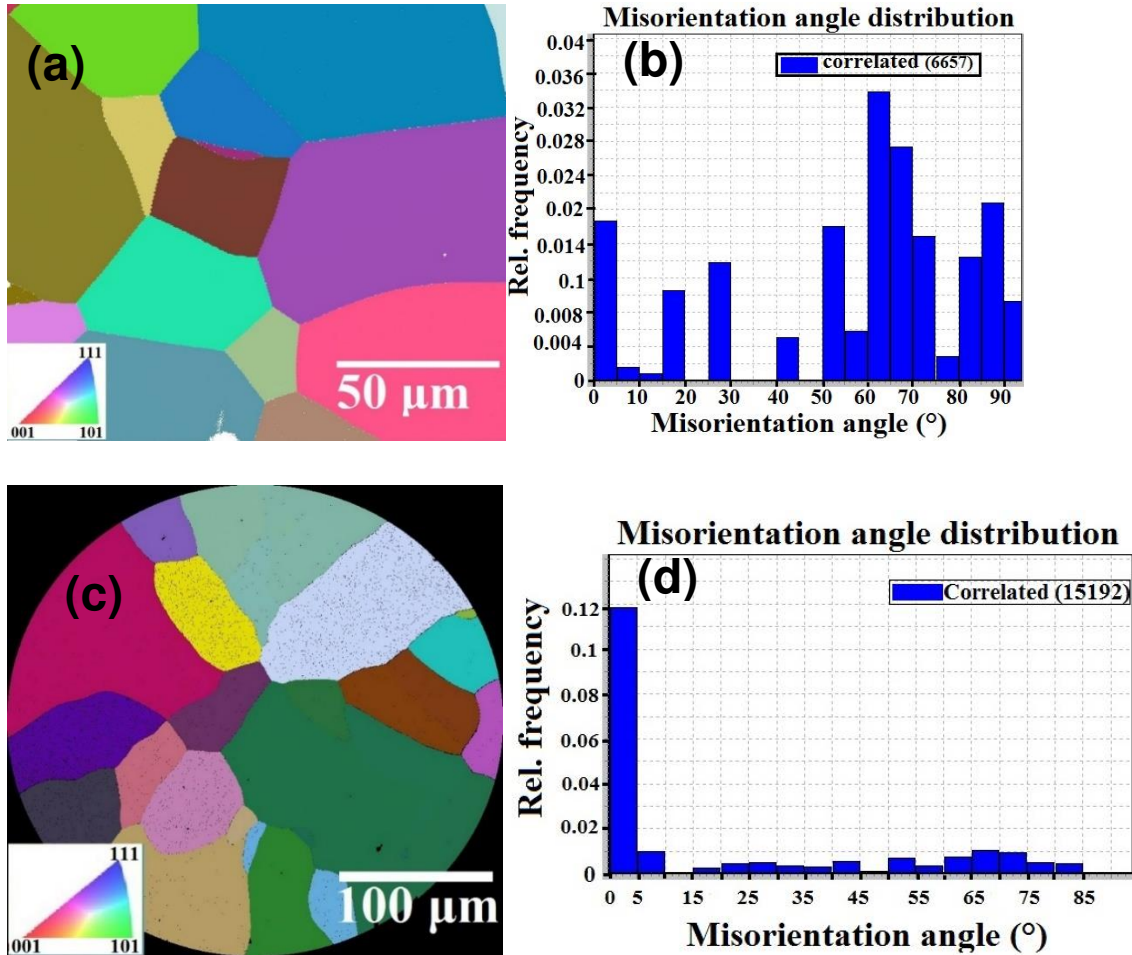


Figure 4: (a & c) shows EBSD results of Euler texture map of unetched Ni_5Ge_3 drop-tube particles from the $> 850 \mu\text{m}$ particle size (partial plate & lath structure) and $300 - 212 \mu\text{m}$ size (complete plate & lath structure) respectively and (b & d) shows the histogram of the correlated misorientation angle distribution across grain boundaries for the images shown in (a & c).

In order to understand the origin of morphologies (partial plate & lath and complete plate & lath morphologies) revealed by etching in the rapidly solidified Ni_5Ge_3 drop-tube samples TEM imaging and selected area diffraction (SAD) analysis has been performed and results of partial plate & lath morphology are shown in the **Figure 5** and the results of complete plate & lath morphology are shown in [15].

We note firstly, that the indexing of the TEM-SAD pattern as shown in Figure 5, confirms the XRD identification, reported above, of this sample as being ϵ' . Moreover, it is only in the featureless matrix materials that the super-lattice spots are apparent (**Figure 5b**). These spots appear far away from the partial plate & lath as well as from the complete plate & lath structures. Interestingly, there are two kinds of superlattice spot observed in Ni_5Ge_3 compound. Double superlattice spot observed in the partial plate & lath structure which can be clearly seen in the **Figure 5b** and single superlattice spots as observed by [] for the ordered variant of the ϵ -phase. From the above phase identification, we may conclude that the double superlattice reflections shown in **Figure 5b** are characteristic of the monoclinic ϵ' -phase, while the single superlattice reflections are characteristic of the hexagonal ϵ -phase. However, consideration of the difference in chemical ordering between the ϵ and ϵ' structures resulting in single and twin sets of superlattice spots is beyond the scope of this paper, here we note only that both indicate the featureless matrix material is chemically ordered. In contrast, if the super-lattice spots are not apparent in the SADP of either the partial plate & lath or the complete plate & lath regions, then it indicates that the material is chemically disordered (**Figure 5c**). Therefore, it is possible to conclude that the contrast revealed by the etching is due to a chemical ordering that is incomplete. In this case, the etchant affects the disordered material and leaves intact the ordered material. Similar behaviour also has been observed in the compound Ni_3Ge [16, 17] and is consistent with the known chemical resistance of ordered intermetallic compounds.

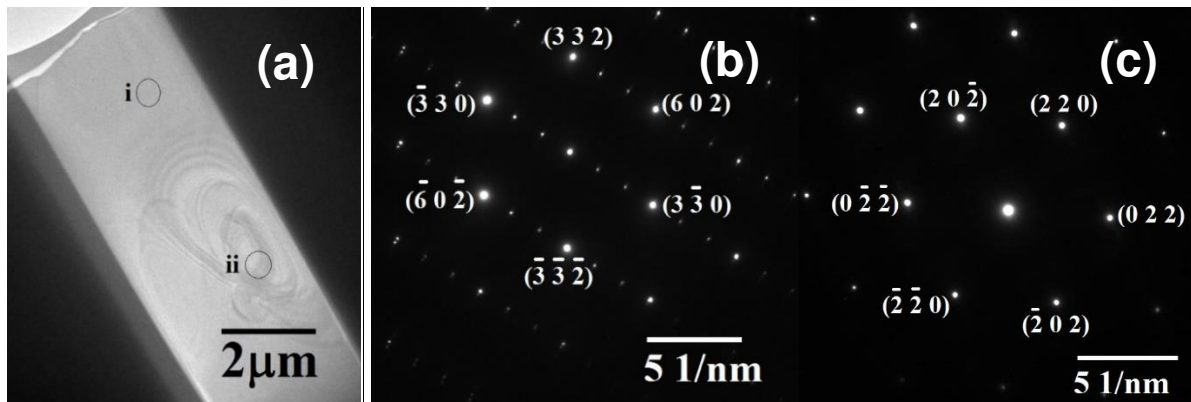


Figure 5: (a) TEM bright field image of a plate & lath structure and surrounding matrix material in a $> 850 \mu\text{m}$ size fraction, (b and c) selected area diffraction patterns from regions (i) and (ii)

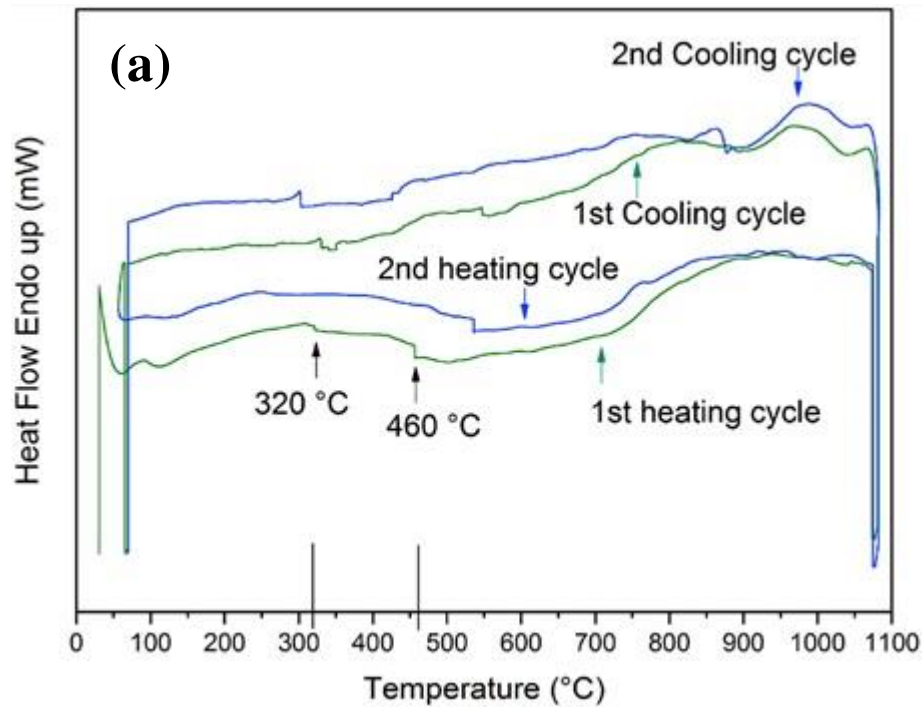
identified in the bright field image (i) matrix materials well away from the partial plate & lath structure, (ii) inside the structure.

Ni_5Ge_3 is a congruently melting compound with a homogeneity range of 34.6 – 44.5 at. % Ge for the single-phase compound. The Ge-deficient end of this range at 37.2 at. % Ge and 1458 K is where the congruent point is located. Ni_5Ge_3 has two equilibrium crystalline forms, ϵ and ϵ' [8] [7]. ϵ' is the low temperature phase with a C2 crystal structure (Monoclinic, space group 5). In contrast, ϵ is the phase of high temperature. It has a $\text{P6}_3/\text{mmc}$ crystal structure (Hexagonal, space group 194) [7]. The transition between the two occurs either congruently ($\epsilon \rightarrow \epsilon'$) at 670 K for Ge-rich compositions or via the eutectoid reaction $\epsilon \rightarrow \epsilon' + \text{Ni}_2\text{Ge}$ at 560 K for Ge-deficient compositions. The phase diagram does not show order-disorder transitions. Furthermore, there is no evidence (apart from this study), as far as we know, as to whether the high temperature ϵ phase orders directly from the liquid or below the liquidus temperature via a solid-state transformation.

So as to determine if the ordering process happens in the solid-state or upon solidification at the liquidus temperature, differential scanning calorimetry (DSC) was used (**Figure 6a**). The results show that two low temperature transformations are evident. As anticipated for materials at 37.2 at. % Ge, we can see from the phase diagram that the first transformation is likely to be the $\epsilon \rightarrow \epsilon' + \text{Ni}_2\text{Ge}$ eutectoid as it appears to be 300 – 320 °C. Interestingly, the largest drop-tube sieve fraction, powders > 850 μm , are characterized as being single phase ϵ' . This indicates that the system was forced to go through the congruent $\epsilon \rightarrow \epsilon'$ transition by a cooling process that was rapid enough to suppress the $\epsilon \rightarrow \epsilon' + \text{Ni}_2\text{Ge}$ eutectoid. The second low temperature transition that is apparent in the DSC is different. It is shown to be 460 – 540 °C, which could be associated to an order-disorder transformation that would have occurred in the high temperature ϵ -phase.

In order to acquire a confirmation of this, an in situ heating experiment was conducted in the TEM. A region that was initially ordered was chosen. This corresponded to the featureless matrix material. It also corresponded to the already identified SAD pattern so as to ensure that the material was ordered (**Figure 6b**). A heating process was used in a progressive manner until the point when the super-lattice spots had vanished entirely. This indicated that the material had changed entirely to the disordered phase (**Figure 6c**). By then, the temperature had reached 485 °C and in agreement with the peak that was shown in the curve of the DSC.

As a consequence, it is apparent that in the Ni-37.5 at.% Ge compound, the disordered variant of the high temperature ϵ -Ni₅Ge₃ phase constitutes the primary solidification phase. In the cooling process, there would be an expectation that this primary solidification phase would go through a solid-state transformation from disordered to ordered at approximately 485 °C. However, it also shows that ordering could be partially suppressed via cooling at rates in excess of 700 K s⁻¹. The suppression of a change to ϵ' would also occur at these cooling rates, in turn, this would result in ϵ that is retained and metastable at room temperature. Additionally, it is apparent that the suppression of low temperature ϵ' -phase transformation does not occur for cooling rates below 700 K s⁻¹. This suppression could be brought about forcefully through the $\epsilon \rightarrow \epsilon'$ transition that is congruent instead of the $\epsilon \rightarrow \epsilon' + \text{Ni}_2\text{Ge}$ eutectoid reaction.



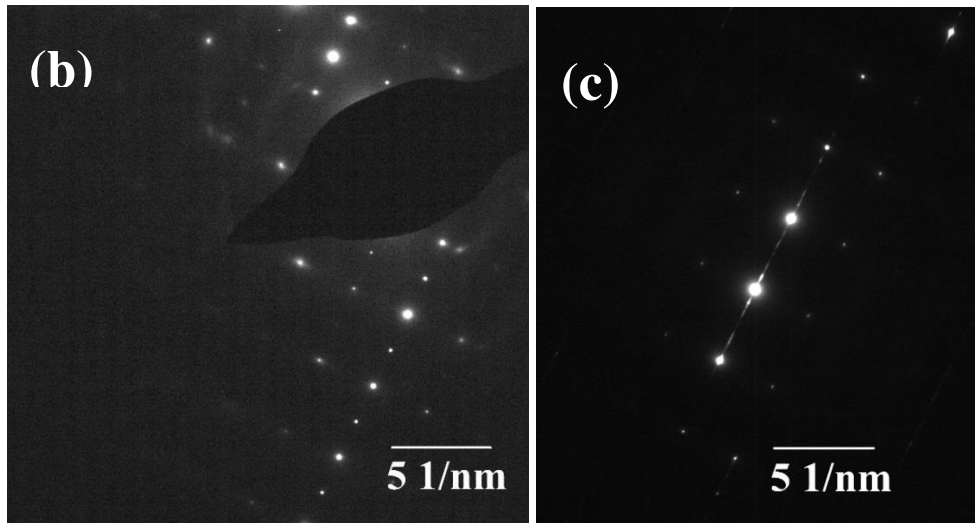


Figure 6 (a) DSC trace from a Ni_5Ge_3 drop-tube particle from the 150 – 106 μm size fraction, 1st and 2nd cycle indicated by green and blue respectively, two vertical black line shows the transition temperature at 320 to 460 $^\circ\text{C}$ and (b) TEM (In-situ) SAD pattern taken from featureless matrix at room temperature (ordered) and (c) SAD of the same area but at 485 $^\circ\text{C}$ (disordered).

These results raise an additional question that relates to why Ni_5Ge_3 compound simultaneously displays ordered and disordered regions when such ordering is occurring via a solid-state reaction. In a previous paper we showed that Ni_3Ge also showed a mix of ordered and disordered regions [1]. However, Ni_3Ge orders direct from the liquid and in this case the explanation was that the disordered compound formed during the rapid, recalescence phase of solidification, while slower post-recalescence growth gave rise to the ordered compound. Of course, in Ni_5Ge_3 such an explanation is not tenable because, as shown above, ϵ disorders above 485 $^\circ\text{C}$. However, such an observation is consistent with solid-state ordering, if such ordering occurs via a first order transformation. Both first and second order ordering reactions can show partial ordering, but these are of a different character. In a 2nd order transformation, partial ordering means all the material shows some degree of partial order (i.e. with order parameter, $\eta < 1$). In contrast, 1st order partial ordering means some regions are fully ordered and some disordered. This is possible due to the transformation proceeding via a nucleation and growth mechanism. In this case rapid cooling would suppress either the nucleation or (more likely) the growth stage of the ordering reaction, leading to the observed mixed morphology of ordered and disordered regions.

In contrast, the suppression of a spontaneous, second order, ordering could not occur in this way and would not give rise to the observed mixed morphology of ordered and disordered regions.

3. Summary & Conclusion

The congruently melting, single phase, intermetallic compound ϵ -Ni₅Ge₃ (T_m = 1185 °C), of composition Ni-37.2 % Ge, was successfully produced and then the compound was subjected to rapid solidification via drop-tube processing. During such processing the compound remains fully single phase ϵ -Ni₅Ge₃/ ϵ' -Ni₅Ge₃, irrespective of the imposed cooling rate. Rapid solidification of the congruently melting intermetallic compound ϵ -Ni₅Ge₃ has revealed a range of solidification microstructures, imbedded within a featureless matrix. The solidification microstructure, which evolve with increasing departure from equilibrium are as follows:

- (i) Partial plate and lath microstructure ($d > 850 \mu\text{m}$, $< 700 \text{ K s}^{-1}$),
- (ii) Plate and lath microstructure ($d = 850 - 150 \mu\text{m}$ diameter particles, $700 - 7800 \text{ K s}^{-1}$)

In the lowest cooling rate $< 700 \text{ K s}^{-1}$, ($d > 850 \mu\text{m}$) the low temperature ϵ' -phase was observed, as expected, upon cooling to room temperature, albeit that the eutectoid formation of the Ni₂Ge compound was suppressed. The dominant solidification morphology, revealed after etching, is that of isolated partial plate and laths within a featureless matrix. In all powder sizes except the largest sieve fraction ($d > 850 \mu\text{m}$) the high temperature ϵ -phase was found to be retained upon cooling to room temperature. Selected area diffraction analysis in the TEM reveals that the partial plate and laths and plate and laths are the disordered variant of ϵ' -Ni₅Ge₃ and ϵ -Ni₅Ge₃ respectively, whilst the featureless matrix of both microstructures are the ordered variant of the same compound.

Differential scanning calorimetry (DSC) indicates two low temperatures transformations. The first of these appears between 300 – 320 °C and is likely to be the $\epsilon \rightarrow \epsilon' + \text{Ni}_2\text{Ge}$ eutectoid decomposition. The second appears to be in the range 460 – 540 °C and we postulate may be associated with the order-disorder transformation in the high temperature ϵ -phase. An in situ heating in the TEM also indicated a solid-state order-disorder transformation between 470 - 485 °C, with the material transforming to the fully disordered phase above 485 °C. When DSC data and an in situ heating in the TEM analysis is combined with microstructural analysis, it is possible to conclude that for Ni₅Ge₃ ordering takes place via a first order solid-state transformation, which can be partially suppressed by rapid cooling. Moreover, as the ordered variants of both compounds

are more resistant to chemical attack than the disordered variants, the morphology of the disordered regions can be revealed by using an aggressive (HF-based) etch.

Acknowledgments

Nafisul Haque is thankful to the Higher Education Commission (HEC) Pakistan and NED University of Engineering & Technology for financial support.

References

- [1] W. Kurz, 50 Year's Solidification Research : The Dendrite Growth Problem between Brighton and Old Windsor, Proceedings of the 5th Decennial International Conference on Solidification Processing, Old Windsor, (July 2017) 1-12.
- [2] P. Duwez, R. Willens, W. Klement Jr, Continuous series of metastable solid solutions in silver- copper alloys, Journal of Applied Physics, 31 (1960) 1136-1137.
- [3] H. Jones, Effects of Experimental variables in rapid quenching from the melt. In rapidly quenched metals, MIT Press Journals, (1975) 1-27.
- [4] W. Boettinger, S. Coriell, R. Sekerka, Mechanisms of microsegregation-free solidification, Materials Science and Engineering, 65 (1984) 27-36.
- [5] A. Taub, M. Jackson, Mechanical Properties of Rapidly Solidified Nickel-Base Superalloys and Intermetallics, MRS Online Proceedings Library Archive, 58 (1985).
- [6] S. Kang, P.K. Domalavage, N.J. Grant, Mechanical properties of rapidly solidified modified cupro-nickel alloys, Materials Science and Engineering, 78 (1986) 33-44.
- [7] S. Jin, C. Leinenbach, J. Wang, L.I. Duarte, S. Delsante, G. Borzone, A. Scott, A. Watson, Thermodynamic study and re-assessment of the Ge-Ni system, Calphad, 38 (2012) 23-34.
- [8] A. Nash, P. Nash, The Ge- Ni (Germanium-Nickel) system, Journal of Phase Equilibria, 8 (1987) 255-264.
- [9] M. Hyman, C. McCullough, J. Valencia, C. Levi, R. Mehrabian, Microstructure evolution in TiAl alloys with B additions: conventional solidification, Metallurgical Transactions A, 20 (1989) 1847.
- [10] C. McCullough, J. Valencia, C. Levi, R. Mehrabian, Microstructural analysis of rapidly solidified Ti-Al-X powders, Materials Science and Engineering: A, 124 (1990) 83-101.
- [11] T. Broderick, A. Jackson, H. Jones, F. Froes, The effect of cooling conditions on the microstructure of rapidly solidified Ti-6Al-4V, Metallurgical Transactions A, 16 (1985) 1951-1959.
- [12] G. Krauss, A. Marder, The morphology of martensite in iron alloys, Metallurgical and Materials Transactions B, 2 (1971) 2343-2357.
- [13] A. Nash, P. Nash, Binary Alloy Phase Diagrams, in: US National Bureau of Standards Monograph Series 25, Elsevier, ASM, Ohio, 1976, pp. 35.

- [14] N. Haque, R.F. Cochrane, A.M. Mullis, The Role of Recrystallization in Spontaneous Grain Refinement of Rapidly Solidified Ni₃Ge, *Metallurgical and Materials Transactions A*, 48 (2017) 5424-5431.
- [15] N. Haque, R.F. Cochrane, A.M. Mullis, Order-disorder morphologies in rapidly solidified ϵ/ϵ' -Ni₅Ge₃ intermetallic, *Journal of Alloys and Compounds*, 739 (2018) 160-163.
- [16] N. Haque, R.F. Cochrane, A.M. Mullis, Disorder-order morphologies in drop-tube processed Ni₃Ge: Dendritic and seaweed growth, *Journal of Alloys and Compounds*, (2016).
- [17] N. Haque, R.F. Cochrane, A.M. Mullis, Morphology of Order-Disorder Structures in Rapidly Solidified L12 Intermetallics, in: *TMS 2017 146th Annual Meeting & Exhibition Supplemental Proceedings*, Springer, 2017, pp. 729-736.